Symmetry in the Ka-band Correlation Receiver's Input Circuit and Spectral Baseline Structure

NRAO GBT Memo 248

June 7, 2007

A. Harris[a,b], S. Zonak[a], G. Watts[c]

[a]University of Maryland; [b]Visiting Scientist, National Radio Astronomy Observatory; [c]National Radio Astronomy Observatory, Green Bank

Abstract

We find that changing the Ka-band receiver's present asymmetrical input circuit to a symmetrical form will improve the spectral baselines and receiver stability by a useful amount. Although we used the Zpectrometer for the measurements, the problem we find lies in the receiver, and affects observations with all backends.

1 Introduction

These notes describe measurements that explore the origin of the the Ka-band correlation receiver's troublesome spectral baselines[1]. Although we used the Zpectrometer for the measurements, the problem we find lies in the receiver, and affects observations with all backends. After Zpectrometer commissioning spectroscopy in Fall 2006, we had proposed that differential loss between the receiver's two inputs was important in producing strong baseline structure. A detailed account is in [1]. Briefly, an ideal correlation spectrometer has an output u

$$u \propto \alpha\beta(T_X - T_Y)g_A g_B^* g_M , \qquad (1)$$

proportional to the power differences between its inputs X and Y, multiplied by hybrid, amplifier, and multiplier gains. A correlation receiver is more stable than a total-power receiver when T_X and T_Y are identical, each with the same contributions from receiver and sky noise. Small gain fluctuations then have a negligibly small signal to multiply, adding negligibly little offset (but perhaps causing a small calibration error for an astronomical source's intensity). It is straightforward to extend the ideas behind Equation (1) for cross-correlation backends for spectroscopy.

The problem we found in Fall 2006 was that some amplitudes in the cross-correlation functions were far from zero. The zero-lag (total power) offset had been trimmed to be small, but offsets at other low lags produced considerable spectral baseline structure across the receiver's band. Gain fluctuations acted on the offsets to produce time-variable baselines. Nodding the telescope so the source was first in one beam, then the other, removed much of the baseline structure but still left residuals in the spectra.

We are taking two approaches to reducing the baseline structure: minimizing the offsets and improving the gain stability. Here we discuss measurements that show that differential loss in the receiver's input circuitry is the main culprit in generating cross-correlation offsets.

---

[1]GBT Memo 249, "Basic Stability of the Ka-band Correlation Receiver," describes subsequent related work.
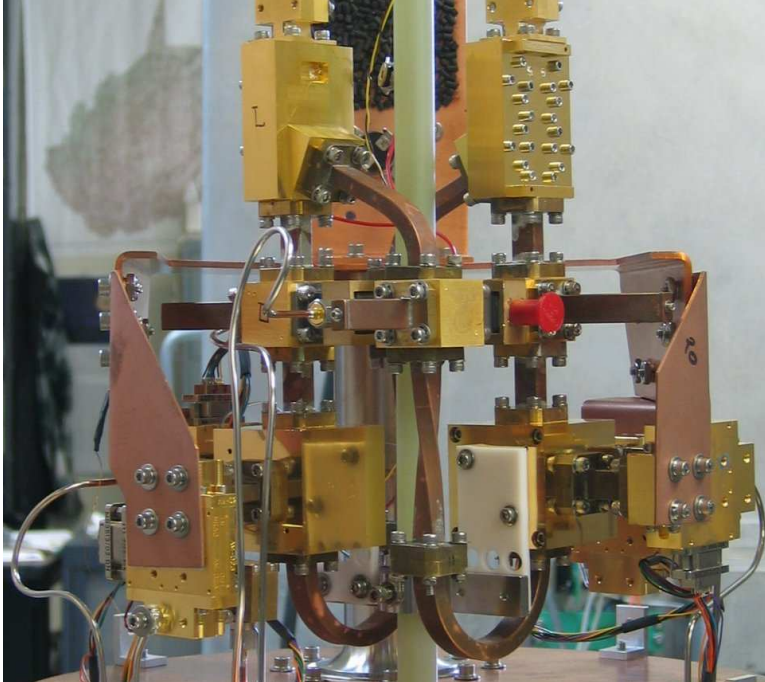
Figure 1: Photograph of the asymmetrical front end's input circuitry showing the OMTs, calibration couplers, input hybrids, and amplifiers. The Zpectrometer connects to the circuitry on the right hand side of this view. For scale, the hybrid is a 1.5″ cube held in place by the white bracket.

2   Results

All of the measurements we report here were made in the Green Bank lab from May 29 through June 1, 2007. We used three of the Zpectrometer's four bands, denoted Slots 1 through 3, covering the top end of the receiver band. We analyzed the data with a set of scripts in the R language [2].

2.1   The asymmetric receiver

We started with the receiver as it was on the GBT through winter 2006/2007, except that it was warm. We recorded cross-correlation functions (CCFs) as we systematically dismantled the input circuit. Figure 1 shows the lower section of the circuitry, a compact design optimized to fit all the components needed for full dual-polarization operation into a small volume. One port of the input hybrid connects to the through port of an orthomode transducer (OMT) through short sections of waveguide and a cross-guide coupler for calibration signals; the other port connects to the side port of the other OMT through a 30° bend, calibration coupler, 90° twist, and 180° bend. In addition to characterizing the offsets as we removed components, where the receiver contains paired components, such as the horn and polarizer assemblies, we exchanged the components to separate the effects of individual parts from systemic interactions.

Our measurements establish that differential loss between the inputs is indeed the origin of the baseline structure. Table 1 summarizes measurements of the effect of removing or exchanging components, here recorded for Slot 2, one of the Zpectrometer bands in the center of the receiver band. An appendix contains similar tables for Slots 1 and 3, but the basic results

Description	CCF rms	CCF min	CCF max	File
Full receiver	1.00	1.00	1.00	13001.tpr
Radome off	0.96	0.96	0.96	13016.tpr
Zotefoam window off	0.93	0.87	0.98	13022.tpr
Vacuum jacket, radiation shield off	0.90	0.84	0.94	13031.tpr
Exchange horns and polarizers	0.88	0.81	0.91	13037.tpr
Remove OMT	0.12	0.10	0.09	13046.tpr
Remove cross-guide couplers	0.10	0.11	0.06	13052.tpr
Terminate at hybrid	0.05	0.05	0.04	13061.tpr
Terminate at amplifiers	0.04	0.05	0.03	13070.tpr

Table 1: Summary of the Slot 2 (32.6–36.1 GHz) CCF structure changes as components are removed and exchanged. The values are normalized to those for the full receiver.

do not change. Exchanging components changed the CCFs by only small amounts, showing that reflection loss dominates over mismatched ohmic loss in individual components. This result is consistent with the observation that the CCFs' structures, with both horns viewing a laboratory-temperature load, change very little whether the receiver is cold or warm. It is also consistent with our discussion of offsets measured with the cold receiver, which were not in thermal equilibrium with the physical temperatures [1].

Removing the orthomode transducers causes the most dramatic reduction in structure, as measured by extreme values and the root mean square (rms) amplitude across lags. Loss in the OMTs is unlikely to be the problem: exchanging the two had little effect, and previous network analyzer measurements have shown that their losses are well-matched. It is more likely that reflections from impedance mismatch and additional path length interact with the surrounding components to produce the structure.

2.2 A proof-of-concept balanced front end

We assembled a full prototype front end with the simplest possible circuit, shown in Figure 2. In addition to incorporating as much symmetry as possible, this circuit eliminates the OMTs, a major cause of the CCF structure. With the pair of bends on hand, the spacing between the horns increases from 75 mm to about 95 mm, corresponding to a beam separation of about 2.3′.

3 COMPARISON OF ASYMMETRICAL AND SYMMETRICAL INPUT CIRCUITS

Figure 3 is a comparison of raw spectra from the receiver in its original asymmetrical and the prototype symmetrical configurations. We emphasize that the spectra are very raw: they include structure from the amplitudes of the calibration tone, and the inversion transforms are from November 2006 data for the cooled receiver. The spectra do provide an impression of the possible improvements by changing from an asymmetrical to a symmetrical receiver, however.

For quantitative comparisons, the raw CCFs are considerably more useful, as no calibration is necessary. Tying together improvements in the lag and spectral domains, Rayleigh's theorem for Fourier transforms [3] shows that the rms in the spectral baselines scales with the rms in the lag domain. Figure 4 contains the measured CCFs for Fig. 3. Lag increases to the left and the zero lag is near the right hand side of the plots. As measured by either the rms or extreme
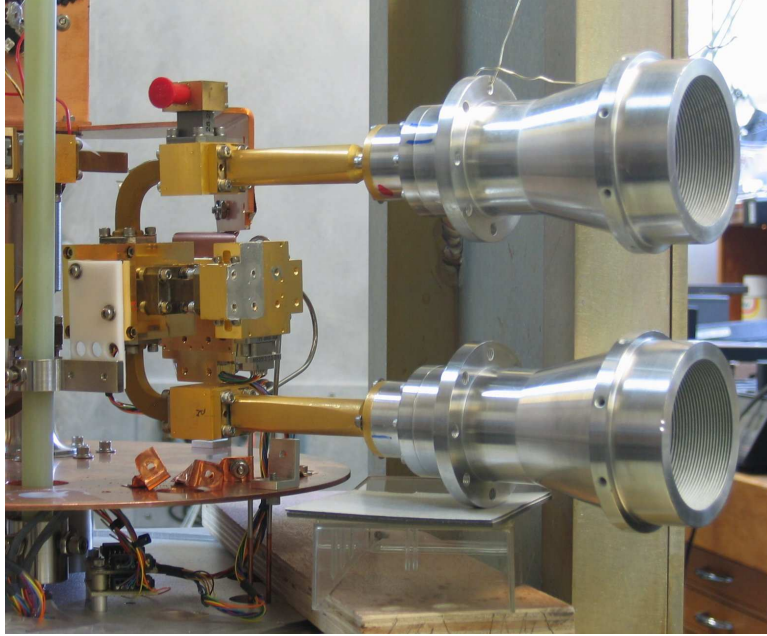
Figure 2: Photograph of the prototype symmetrical front end.

values, the structure amplitudes are factors of 3 to 6 lower for the symmetrical than for the asymmetrical setup.

In addition to showing lower amplitudes for the symmetrical circuit, the spectra give an impression that the baseline structure is somewhat smoother. This would be important for finding lines that might otherwise appear on a sharp edge in the spectrum. Figure 5 contains the same data as Fig. 4 on an expanded scale, showing the reduction of power at high lags that produces edges and steep slopes. The rms in the high lags is a factor of 2–3 lower for the symmetrical input stage than for the asymmetrical arrangement. In general, comparing the CCFs shows that the symmetrical circuit CCF has fewer components, especially at higher lags, than the asymmetric circuit.
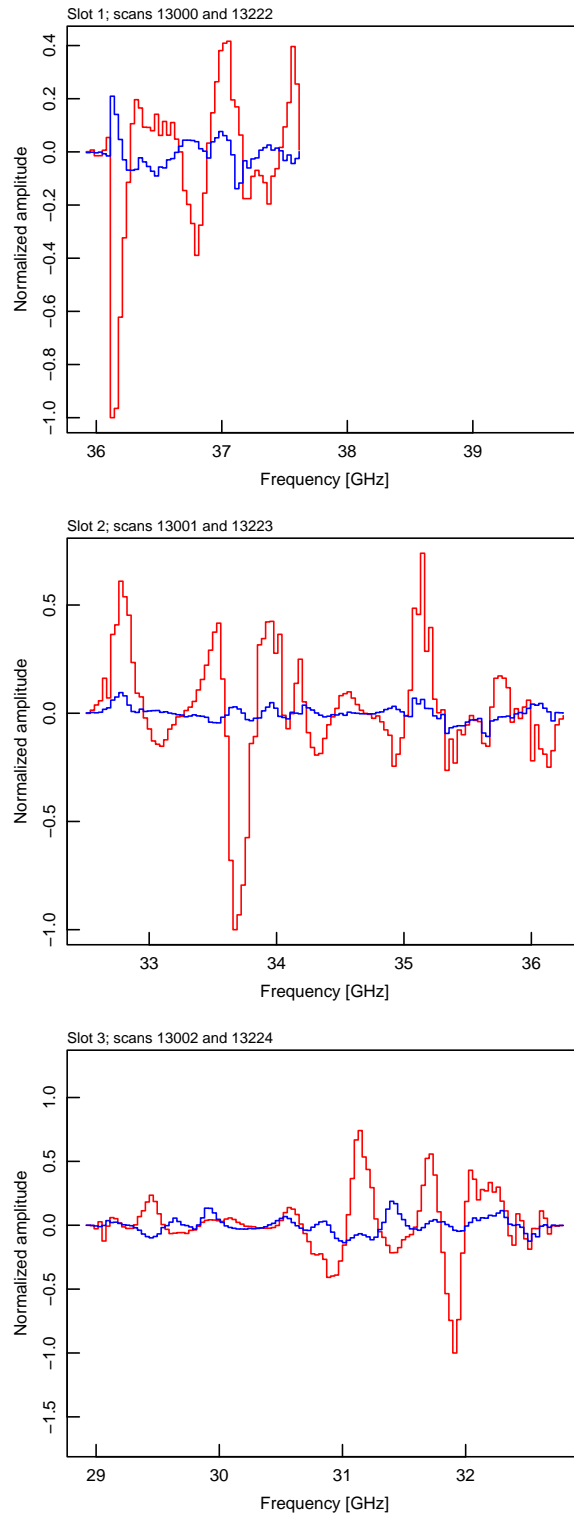
Figure 3: Raw spectra with the asymmetrical and symmetrical front end circuitry give an impression of the effect of changing from an asymmetrical to a symmetrical input circuit. Red denotes the asymmetrical case, blue the symmetrical.
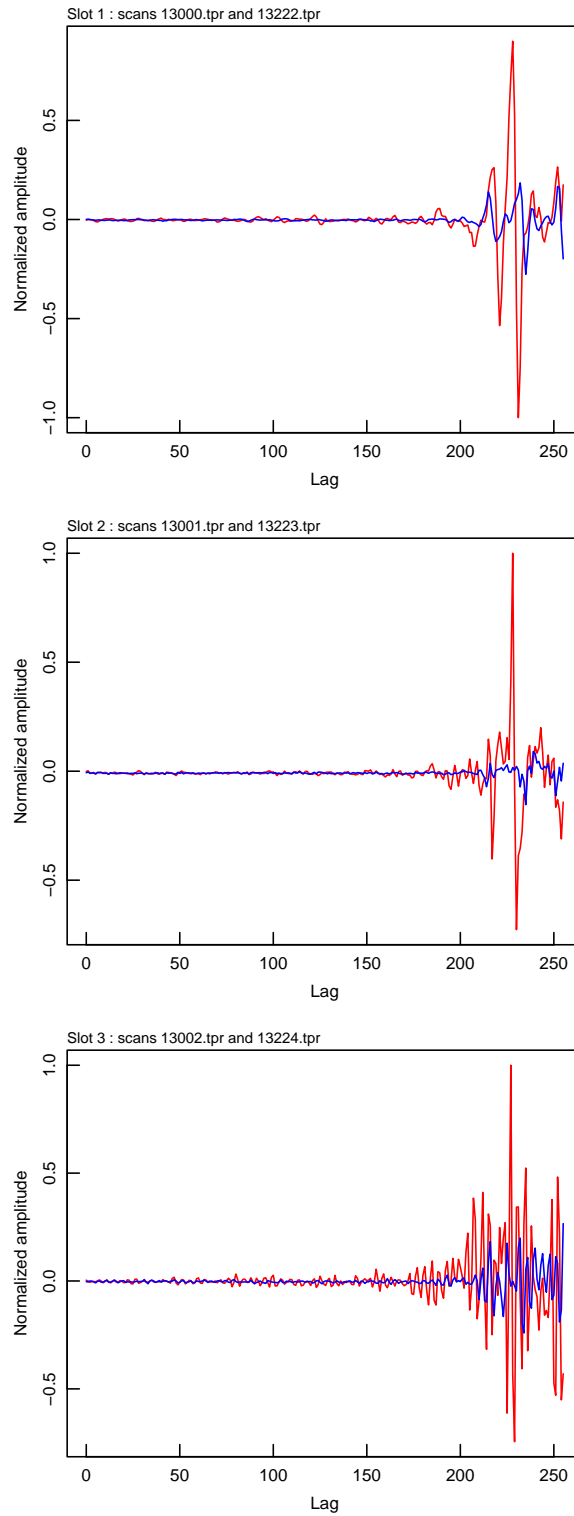
Figure 4: Cross-correlation functions with for the asymmetrical and symmetrical front end circuitry. Red denotes the asymmetrical case, blue the symmetrical. High lags are at toward the left, with the total power lag near the right-hand edge of the plot.
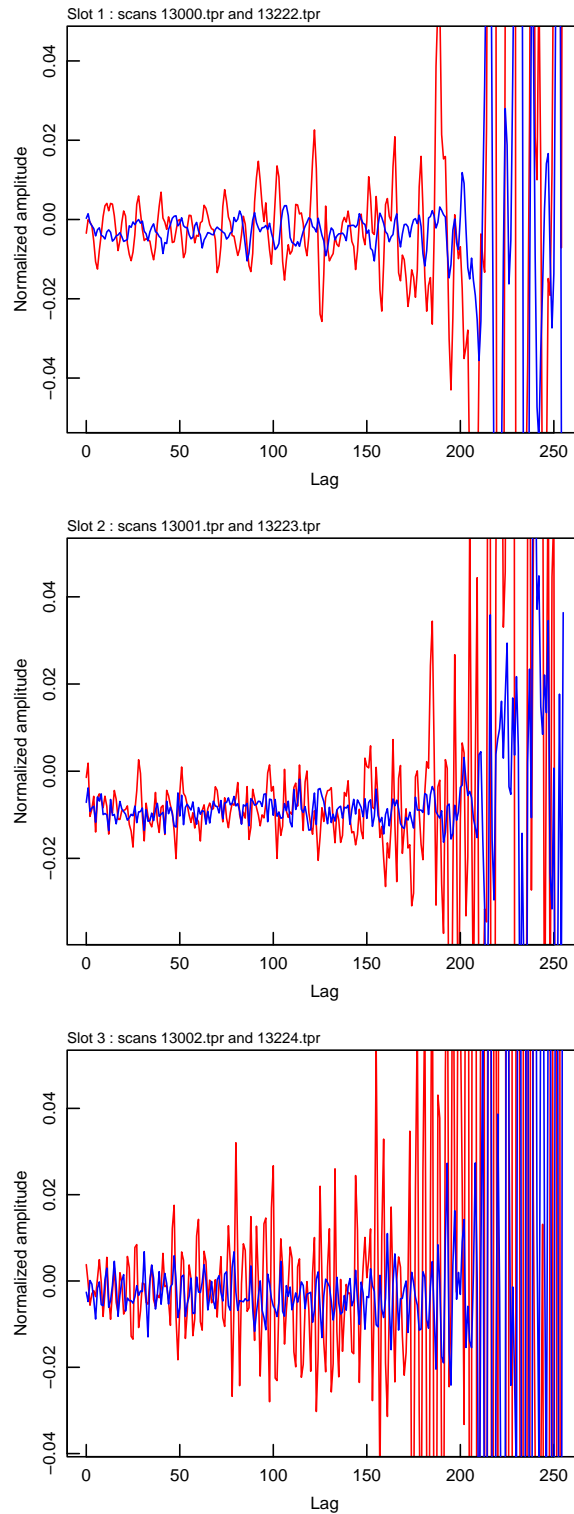
Figure 5: Cross-correlation functions with for the asymmetrical and symmetrical front end circuitry, on an expanded scale to show the structure at high lags. Red denotes the asymmetrical case, blue the symmetrical.

4 CONCLUSIONS AND IMPLICATIONS

We have shown that the input circuit has a strong effect on the quality of the spectral baselines for the Ka-band receiver. This is a fundamental result that applies to all correlation receivers and corresponding backend spectrometers.

Changing to a symmetrical input circuit carries clear benefits for spectroscopy with the Ka-band receiver. In a broader sense, the main cost is the loss of the second polarization, which would cause a theoretical penalty of a factor of two with some backends. The factor two advantage is quite theoretical in practice for many observations: the present baseline problems prevent the theoretical gain from the additional polarization from being useful for deep integrations in lines or continuum. In addition, a dual-channel's system temperatures must also be well matched to reach the theoretical time advantage of two. To reach the same signal to noise ratio, the integration time ratio for a single to double-channel receiver depends on the relative noise temperatures in the two channels as

$$\frac{\tau_s}{\tau_d} = \frac{4p^2}{1+q^2} \; ,$$

(2)

where p is the ratio of the single-channel system temperature to the lower of the two dual-channel system temperatures, and $q \geq 1$ is the ratio of the higher to lower dual system temperatures. For all amplifier temperatures equal, the single-channel system must integrate twice as long as the dual-channel system. The advantage drops rapidly as the second channel becomes noisier. Equation (2) shows a drop from 2 to 1.33 when the higher-noise channel is $\sqrt{2}$ noisier than the other channel ($q = \sqrt{2}$, $p = 1$). A small reduction in input loss with a simpler circuit is unlikely to provide a significant improvement in receiver temperature for the single-channel system compared with the dual channel system.

Reducing the structure in the CCFs will increase the receiver's stability (see Eq. (1)) by reducing the amount of power from gain fluctuations relative to the radiometric noise. We earlier [1] derived an expression linking the coefficient of drift component variance to the minimum Allan variance time,

$$T_{min} = \left(-\frac{\beta b}{\alpha a} \right)^{1/(\alpha - \beta)} .$$

(3)

Here a is the variance at 1 s integration time, α is the power law for the radiometric term, and b and β are the equivalents for the drift term. b, a coefficient for a variance term, scales as the square of the instability's amplitude, which we estimate from the CCF rms. T_{min} scales as approximately $b^{0.4}$ for typical measured values of α and β. The time to the minimum in the Allan variance therefore scales nearly linearly with the rms of the CCFs. Reducing the structure rms by a factor of 3–6, as we measure with the symmetrical receiver, should increase the stability time by a similar factor. With Fall 2006 Allan variance minimum times of 5–10 s and plans to decrease the nodding time, either by improving software efficiency or by nodding with the subreflector, the potential improvement is very useful.

Both feed horns in the proof-of-concept prototype (Figure 2) have the same polarization, and we are investigating adding 45° twists with opposite handedness to the signal path to cross-polarize the inputs. This would reduce the sensitivity to atmospheric emission. A correlation receiver with a 180° hybrid detects the cross-product of the voltages x and y at the inputs as $(\alpha^2 - \beta^2)\langle xy \rangle$ [4], with rejection depending on the hybrid's power match (α and β have different meanings here than in the previous paragraph) to suppress the atmospheric emission. A 55-45 hybrid power split gives $\alpha^2 - \beta^2 = 0.1$, or 10 dB rejection, for example. It remains to be seen

whether an improvement in atmospheric rejection would be offset by structure introduced by adding twists.

Separating the beams somewhat beyond the present $1.8'$ will not substantially affect the beam overlap through the atmosphere, so the atmospheric common-mode rejection should change little. Changing the separation from $1.8'$ to about $2.3'$ as an example, changes the altitude at which the beam centers separate by 10 m from 19 km to 12 km, which is essentially at the top of the troposphere. Larger separations should be possible, since most of the water is at altitudes below 10 km. Procuring bends with larger radii would likely reduce the structure in the CCF further, as the reflections could be expected to be lower.

The amount of work needed to rebuild the receiver as a single channel, symmetrical system is not large. The main tasks are new brackets for circuit components and a perhaps new radiation shield and cryostat vacuum tops. It should be possible to complete this work on the timescale of a few months if modest resources are dedicated to the task. Accommodating co- and cross-polarization components and experimenting with different beam separations would add of order a month to the development.

REFERENCES

[1] A. Harris, S. Zonak, K. Rauch, A. Baker, G. Watts, K. O'Neil, R. Creager, B. Garwood, and P. Marganian, "Zpectrometer commissioning report, Fall 2006." NRAO Green Bank Telescope memo series No. 245, 2007. http://wiki.gb.nrao.edu/bin/view/Knowledge/GBTMemos.

[2] R Development Core Team, *R: A Language and Environment for Statistical Computing.* R Foundation for Statistical Computing, Vienna, Austria, 2006. http://www.R-project.org.

[3] R. Bracewell, *The Fourier Transform and its Applications.* McGraw-Hill, second ed., 1986.

[4] A. Harris, "Spectroscopy with multichannel correlation radiometers," *Rev. Sci. Inst.*, vol. 76, pp. 4503–+, May 2005.

Description	CCF rms	CCF min	CCF max	File
Full receiver	1.00	1.00	1.00	13000.tpr
Radome off	0.97	0.97	0.96	13015.tpr
Zotefoam window off	0.96	0.99	0.91	13021.tpr
Vacuum jacket, radiation shield off	0.93	0.95	0.88	13030.tpr
Exchange horns and polarizers	0.90	0.95	0.82	13036.tpr
Remove OMT	0.20	0.21	0.17	13045.tpr
Remove cross-guide couplers	0.16	0.10	0.21	13051.tpr
Terminate at hybrid	0.09	0.09	0.12	13060.tpr
Terminate at amplifiers	0.03	0.04	0.01	13069.tpr

Table 2: Summary of the Slot 1 (nominally 36.1–39.6 GHz) CCF structure changes as components are removed and exchanged. The values are normalized to those for the full receiver.

Description	CCF rms	CCF min	CCF max	File
Full receiver	1.00	1.00	1.00	13002.tpr
Radome off	0.96	0.97	0.96	13017.tpr
Zotefoam window off	0.92	0.98	0.95	13023.tpr
Vacuum jacket, radiation shield off	0.88	0.95	0.93	13032.tpr
Exchange horns and polarizers	0.92	1.10	1.08	13038.tpr
Remove OMT	0.38	0.43	0.32	13047.tpr
Remove cross-guide couplers	0.13	0.17	0.10	13053.tpr
Terminate at hybrid	0.06	0.06	0.08	13062.tpr
Terminate at amplifiers	0.02	0.03	0.02	13071.tpr

Table 3: Summary of the Slot 3 (29.1–32.6 GHz) CCF structure changes as components are removed and exchanged. The values are normalized to those for the full receiver.